AIMS Mathematics, 10(8): 19795–19815.
DOI: 10.3934/math.2025883
Received: 20 June 2025
Revised: 07 August 2025
Accepted: 19 August 2025
Published: 28 August 2025

https://www.aimspress.com/journal/Math

Research article

Efficient Jacobi spectral-IRK method for one- and two-dimensional tempered fractional Allen-Cahn equations

Maged Z. Youssef[1], Mahmoud A. Zaky[1], Faizah A.H. Alomari[2], Amra Al Kenany[3] and Samer Ezz-Eldien[4*]

[1] Department of Mathematics and Statistics, College of Science, Imam Mohammad Ibn Saud Islamic University (IMSIU), Riyadh, Saudi Arabia

[2] Department of Mathematics, Faculty of Science, Al-Baha University, Al-Baha 65779, Saudi Arabia

[3] Mathematics Department, Al-Qunfudah University College, Umm Al-Qura University, Mecca, KSA

[4] Department of Mathematics, Faculty of Science, New Valley University, El-Kharga 72511, Egypt

* **Correspondence:** Email: s_sezeldien@yahoo.com.

Abstract: Tempered fractional Allen-Cahn equations have many vital applications in science and engineering. The presence of a tempered fractional derivative enables these equations to efficiently explain more complex systems where long-range effects exist with an exponential decay. In this paper, we provide a numerical approach to tempered space-fractional Allen-Cahn equations. The spectral collocation method is implemented, based on Jacobi polynomials, to reduce one- and two-dimensional tempered space-fractional Allen-Cahn equations to a system of ordinary differential equations in the time direction. Then, the implicit Runge-Kutta method is applied to approximate the resulting system. This is the first work that uses the implicit Runge-Kutta method to solve one- and two-dimensional tempered space-fractional Allen-Cahn equations. High accuracy of the spectral collocation method, together with the simplicity and low computational cost of the implicit Runge-Kutta method, represent key advantages of the proposed scheme when applied to such a problem. Numerical results for two test problems are performed to test the validity and superiority of the suggested numerical scheme over other numerical schemes.

Keywords: tempered fractional Allen-Cahn equation; Jacobi polynomials; spectral collocation; implicit Runge-Kutta; exponential tempering
Mathematics Subject Classification: 65L05, 65R20, 65N35, 65L03

1. Introduction

The Allen-Cahn equation was initially formulated by Allen and Cahn [1] to analyze the behavior of antiphase boundaries within crystalline solids. The Allen-Cahn equation has since been found to be an important tool to describe many real-world phenomena, such as interface motion, computer vision, multiphase flow, machine learning, and statistical mechanics, see [2–5]. The space-fractional Allen-Cahn equation is a modification of the classical Allen-Cahn equation, which replacing the second-order derivative in the space-direction with an arbitrary-order one, thus enhancing the equation's capability to study the memory effects and anomalous diffusion of a system. Consequently, investigating space-fractional Allen-Cahn equations and finding their numerical solutions have garnered significant attention in the last years. To solve space fractional Allen-Cahn equations, Yin et al. [6] applied the time two-mesh finite element scheme, where the implicit Crank–Nicolson method and second-order backward difference method were used in the time-direction and the finite element method was used in the space-direction. Li et al. [7] introduced the reduced-dimension extrapolation two-grid Crank-Nicolson finite element method. Yuan and Hui [8] proposed a higher-order time-splitting Monte Carlo method by integrating the spectral Monte Carlo method with a time-splitting scheme. Bu et al. [9] introduced a convex splitting method with the Crank–Nicolson approach in the time direction and the Fourier spectral approach in the space direction. Zhang and Yang [10] used a first-order scheme in the time direction and a second-order weighted and shifted Grunwald difference formula in the space direction, additionally they investigated unconditional energy stability and discrete maximum principle preserving schemes. Zhai et al. [11] applied an explicit operator splitting method together with the fourth-order compact difference scheme. Chen et al. [12] established a fully discrete scheme based on the modified Crank-Nicolson scheme in the time direction and the Legendre spectral method in the space direction. Hou et al. [13] considered a fully discretized scheme using the conventional second-order Crank–Nicolson method in the time direction and the second-order central difference method in the space direction. Zhang and Yang [14] performed a linearized two-level approach based on the shifted Grunwald difference scheme in the space direction and the Crank-Nicolson scheme in the time direction, and applied the Newton linearized method for the nonlinear term.

Tempered fractional calculus is a generalization of fractional calculus, which incorporates an exponential tempering parameter, this which helps adapt the decay rate of the memory kernel, thus enhancing the ability to model systems with decay and long-range memory effects, such as geophysical flows [15], groundwater hydrology [16], finance [17], and poroelastict [18]. Zaky [19] studied the existence and uniqueness of a class of tempered fractional differential equations and applied the spectral collocation scheme for its numerical solution. In [20], the existence and uniqueness of the solution of tempered fractional differential equations were investigated using the Banach fixed point theorem, and its stability was proven using the fractional Gronwall inequality. In [21], the authors studied the observability, controllability, and well-posedness of tempered fractional differential equations. Heris and Javidi [22] used the piecewise quadratic interpolation polynomial technique to develop a predictor–corrector technique with uniform and non-uniform meshes to solve tempered fractional differential equations. Zhao [23] considered the tempered fractional Jacobi functions as the basis of the spectral collocation approach for the numerical solution of tempered fractional differential equations. The authors in [24] implemented the sum of

exponentials method as a basis of a high-order compact finite difference method to solve the two-dimensional tempered fractional reaction-advection-subdiffusion equation. Bibi and Rehman [25] constructed a numerical approach for tempered fractional differential equations which utilized a combination of product integration, Lagrange interpolation, and Newton-Cotes quadrature techniques. Partohaghighi et al. [26] proposed a second-order exponential time-differencing finite element method for Riesz-tempered fractional reaction-diffusion equations. In [27], the authors considered the two-dimensional tempered space-fractional Allen-Cahn equation and used a second-order finite difference approach for its numerical solution.

This work aims to provide a numerical solution to one- and two-dimensional tempered space-fractional Allen-Cahn equations. Based on Jacobi polynomials, the spectral collocation approach is used to reduce the main problem to a system of ordinary differential equations in the time direction. Then, the implicit Runge-Kutta method is applied to approximate the resulting system. This is the first attempt where the implicit Runge-Kutta (IRK) method is used to deal with one- and two-dimensional tempered space-fractional Allen-Cahn equations. The main contributions of this paper are as follows:

- A spectral collocation method using Jacobi polynomials is developed for tempered fractional Allen-Cahn equations, thus achieving exponential convergence in space,
- The framework seamlessly integrates exponential tempering parameters to model anomalous diffusion with truncated memory effects,
- An IRK scheme ensures stable and accurate temporal integration for stiff systems arising from spectral discretization,
- The extension to two dimensions preserves spectral accuracy while handling cross-dimensional coupling.

The paper is outlined as follows: Section 2 introduces some basic tools and definitions, Section 3 presents a numerical solution to the one-dimensional tempered space-fractional Allen-Cahn equation using the spectral collocation approach, Section 4 extends the application of the numerical scheme to the two-dimensional tempered space-fractional Allen-Cahn equation, Section 5 discusses the application of the IRK method to the resulting system of ordinary differential equations, Section 6 obtains the numerical results of two test problems to ensure the validity of the presented numerical scheme, and Section 7 provides some concluding remarks.

2. Preliminaries

2.1. Fractional operators

The left Riemann-Liouville (RL) fractional derivative is defined as follows:

$$ {}_0D_x^{\mu} v(x,t) = \frac{1}{\Gamma(n-\mu)} \frac{\partial^n}{\partial x^n} \int_0^x \frac{v(\tau,t)}{(x-\tau)^{\mu-n+1}}\, d\tau, \quad n-1 < \mu < n, \tag{2.1} $$

where $\Gamma(\cdot)$ is the gamma function, n is an integer, and μ is the fractional order.

The right fractional derivative is given by the following

$$ {}_xD_{\ell}^{\mu} v(x,t) = \frac{(-1)^n}{\Gamma(n-\mu)} \frac{\partial^n}{\partial x^n} \int_x^{\ell} \frac{v(\tau,t)}{(\tau-x)^{\mu-n+1}}\, d\tau, \quad n-1 < \mu < n. \tag{2.2} $$

The tempered fractional derivative fundamentally differs from the standard fractional derivative through the incorporation of an exponential tempering parameter $\gamma > 0$. This modification introduces several distinctive properties. The tempering terms $e^{-\gamma x}$ (left derivative) and $e^{\gamma x}$ (right derivative) truncate the heavy tails of the power-law kernel, thus enabling finite moments and an exponential decay of correlations. This contrasts with the standard fractional derivative's power-law decay and infinite moments. Tempered operators model anomalous diffusion with finite jump lengths, thus making them suitable for systems with truncated Lévy flights where standard fractional operators overestimate long-range interactions.

The left RL tempered fractional derivative extends the classical RL derivative by incorporating an exponential tempering factor γ, and is defined as follows:

$$ {}_0D_x^{\mu,\gamma} v(x,t) = \frac{e^{-\gamma x}}{\Gamma(n-\mu)} \frac{\partial^n}{\partial x^n} \int_0^x \frac{e^{\gamma\tau} v(\tau,t)}{(x-\tau)^{\mu-n+1}}\, d\tau, \quad n-1 < \mu < n, \tag{2.3} $$

where $\gamma > 0$ is the tempering parameter that controls the exponential decay.

Similarly, the right RL tempered fractional derivative is defined as follows:

$$ {}_xD_\ell^{\mu,\gamma} v(x,t) = \frac{(-1)^n e^{\gamma t}}{\Gamma(n-\mu)} \frac{\partial^n}{\partial x^n} \int_x^\ell \frac{e^{-\gamma\tau} v(\tau,t)}{(\tau-x)^{\mu-n+1}}\, d\tau, \quad n-1 < \mu < n. \tag{2.4} $$

The variants of the left and right RL tempered fractional derivatives are defined as

$$ \partial_{+x}^{\mu,\gamma} v(x,t) = {}_0D_x^{\mu,\gamma} v(x,t) - \gamma^\mu v(x,t) - \mu\gamma^{\mu-1} \frac{\partial v}{\partial x}(x,t), $$

and

$$ \partial_{-x}^{\mu,\gamma} v(x,t) = {}_xD_\ell^{\mu,\gamma} v(x,t) - \gamma^\mu v(x,t) + \mu\gamma^{\mu-1} \frac{\partial v}{\partial x}(x,t). $$

The fractional diffusion operator, which combines the left and right variants, is defined as follows:

$$ \partial_{|x|}^{\mu,\gamma} v(x,t) = -\frac{1}{2\cos(\mu\pi/2)} \left(\partial_{-x}^{\mu,\gamma} v(x,t) + \partial_{+x}^{\mu,\gamma} v(x,t) \right). $$

2.2. Jacobi polynomials

The Jacobi polynomials $\mathcal{J}_k^{(\alpha,\beta)}(z)$ with parameters $\alpha, \beta > -1$ provide a comprehensive framework for spectral methods, thereby encompassing several classical orthogonal polynomial families as special cases, including the following:

- Legendre Polynomials: Obtained when $\alpha = \beta = 0$:

$$ P_k(x) = \mathcal{J}_k^{(0,0)}(x). $$

  These form the basis for Legendre spectral methods.
- Chebyshev Polynomials (First Kind): Emerge when $\alpha = \beta = -1/2$:

$$ T_k(x) = \frac{2^k k!}{(2k)!} \mathcal{J}_k^{(-1/2,-1/2)}(x). $$

- Gegenbauer/Ultraspherical Polynomials: The symmetric case $\alpha = \beta = \lambda - 1/2$:

$$C_k^{(\lambda)}(x) = \frac{\Gamma(\lambda + 1/2)\Gamma(2\lambda + k)}{\Gamma(\lambda + k + 1/2)\Gamma(2\lambda)} \mathcal{J}_k^{(\lambda-1/2,\lambda-1/2)}(x).$$

The Jacobi polynomials form a complete orthogonal system on the interval $[-1, 1]$. These polynomials are characterized by several fundamental properties.

The recurrence relation for Jacobi polynomials is given by the following:

$$\mathcal{J}_{k+1}^{(\alpha,\beta)}(z) = \left(A_k^{(\alpha,\beta)} z - B_k^{(\alpha,\beta)}\right) \mathcal{J}_k^{(\alpha,\beta)}(z) - C_k^{(\alpha,\beta)} \mathcal{J}_{k-1}^{(\alpha,\beta)}(z), \quad k = 1, 2, \ldots,$$

with the initial polynomials defined as

$$\mathcal{J}_0^{(\alpha,\beta)}(z) = 1, \quad \mathcal{J}_1^{(\alpha,\beta)}(z) = \frac{1}{2}(\alpha + \beta + 2)z + \frac{1}{2}(\alpha - \beta).$$

The coefficients in the recurrence relation are as follows:

$$A_k^{(\alpha,\beta)} = \frac{(2k + \alpha + \beta + 1)(2k + \alpha + \beta + 2)}{2(k + 1)(k + \alpha + \beta + 1)},$$

$$B_k^{(\alpha,\beta)} = \frac{(\beta^2 - \alpha^2)(2k + \alpha + \beta + 1)}{2(k + 1)(k + \alpha + \beta + 1)(2k + \alpha + \beta)},$$

$$C_k^{(\alpha,\beta)} = \frac{(k + \alpha)(k + \beta)(2k + \alpha + \beta + 2)}{(k + 1)(k + \alpha + \beta + 1)(2k + \alpha + \beta)}.$$

The explicit polynomial form of the Jacobi polynomials is expressed as:

$$\mathcal{J}_k^{(\alpha,\beta)}(z) = \sum_{m=0}^{k} \frac{\Gamma(k + \alpha + 1)\Gamma(k + m + \alpha + \beta + 1)}{\Gamma(k + \alpha + \beta + 1)\Gamma(m + \alpha + 1)m!(k - m)!} \left(\frac{z - 1}{2}\right)^m.$$

Jacobi polynomials are orthogonal with respect to the weight function $w^{(\alpha,\beta)}(z) = (1 - z)^\alpha (1 + z)^\beta$ on the interval $[-1, 1]$. The orthogonality relation is as follows:

$$\int_{-1}^{1} \mathcal{J}_k^{(\alpha,\beta)}(z) \mathcal{J}_l^{(\alpha,\beta)}(z) w^{(\alpha,\beta)}(z)\, dz = h_k^{(\alpha,\beta)} \delta_{kl},$$

where the normalization constant $h_k^{(\alpha,\beta)}$ is

$$h_k^{(\alpha,\beta)} = \frac{2^{\alpha+\beta+1}\Gamma(k + \alpha + 1)\Gamma(k + \beta + 1)}{(2k + \alpha + \beta + 1)k!\Gamma(k + \alpha + \beta + 1)}.$$

For polynomial interpolation, the integral of a function $\phi(z)$ weighted by $w^{(\alpha,\beta)}(z)$ can be approximated using the Jacobi-Gauss-Lobatto (JGL) quadrature rule as follows:

$$\int_{-1}^{1} \phi(z) w^{(\alpha,\beta)}(z)\, dz \approx \sum_{j=0}^{\aleph} w_{\aleph,j}^{(\alpha,\beta)} \phi(z_j),$$

where the nodes z_j include the endpoints $z_0 = -1$ and $z_{\aleph} = 1$, and the interior nodes are the zeros of $\partial_z \mathcal{J}_{\aleph}^{(\alpha,\beta)}(z)$ for $j = 1, \ldots, \aleph - 1$. The corresponding weights are as follows:

$$w_{\aleph,0}^{(\alpha,\beta)} = \frac{2^{\alpha+\beta+1}(\beta+1)\Gamma^2(\beta+1)\Gamma(\aleph)\Gamma(\aleph+\alpha+1)}{\Gamma(\aleph+\beta+1)\Gamma(\aleph+\alpha+\beta+2)},$$

$$w_{\aleph,\aleph}^{(\alpha,\beta)} = \frac{2^{\alpha+\beta+1}(\alpha+1)\Gamma^2(\alpha+1)\Gamma(\aleph)\Gamma(\aleph+\beta+1)}{\Gamma(\aleph+\alpha+1)\Gamma(\aleph+\alpha+\beta+2)},$$

$$w_{\aleph,j}^{(\alpha,\beta)} = \frac{1}{(1-z_j^2)^2} \frac{G_{\aleph-2}^{\alpha+1,\beta+1}}{\left(\partial_z \mathcal{J}_{\aleph-1}^{(\alpha+1,\beta+1)}(z_j)\right)^2}, \quad j = 1, \ldots, \aleph - 1,$$

where

$$G_{\aleph}^{\alpha,\beta} = \frac{2^{\alpha+\beta+1}\Gamma(\aleph+\alpha+2)\Gamma(\aleph+\beta+2)}{(\aleph+1)!\Gamma(\aleph+\alpha+\beta+2)}.$$

3. One-dimensional spectral discretization

In this section, we develop a spatial discretization of the following tempered-fractional Allen-Cahn equation using the pseudospectral collocation method with Jacobi polynomial expansions in the spatial direction. We consider

$$\frac{\partial v}{\partial t}(x,t) - \epsilon\, \partial_{|x|}^{\mu,\gamma} v(x,t) = v(x,t) - v^3(x,t) + p(x,t), \quad \text{in } \Omega = (0,\ell), \text{ for } I = (0,T], \tag{3.1}$$

with the following boundary and initial conditions:

$$v(0,t) = v(\ell,t) = 0, \quad \text{for } t \in I, \text{ on } \partial\Omega,$$

$$v(x,0) = g(x), \quad \text{on } \Omega,$$

where $1 < \mu < 2$, $\gamma > 0$ and ϵ is the interface width parameter.

The solution is expressed in terms of unknown variable coefficients $\hat{v}_s(t)$ as follows:

$$v(x,t) \approx \sum_{s=0}^{\aleph} \hat{v}_s(t)\psi_s(x), \quad s = 0, 1, \ldots, \aleph, \tag{3.2}$$

where $\psi_s(x)$ are shifted Jacobi polynomials defined on the physical domain $[0,\ell]$. These basis functions are constructed from standard Jacobi polynomials $\mathcal{J}_s^{(\alpha,\beta)}(\zeta)$ defined on $[-1,1]$ via the following transformation: $\psi_s(x) = \mathcal{J}_s^{(\alpha,\beta)}(\zeta(x))$, where $\zeta(x) = \frac{2x}{\ell} - 1$. The basis functions $\psi_s(x)$ satisfy the following recurrence relation:

$$\psi_0(x) = 1, \quad \psi_1(x) = \frac{(\alpha+\beta+2)\zeta(x) + (\alpha-\beta)}{2},$$
$$\psi_{s+1}(x) = (A_s\zeta(x) - B_s)\psi_s(x) - C_s\psi_{s-1}(x), \quad s \geq 1,$$

where

$$A_s = \frac{(2s+\alpha+\beta+1)(2s+\alpha+\beta+2)}{2(s+1)(s+\alpha+\beta+1)},$$

$$B_s = \frac{(\beta^2 - \alpha^2)(2s + \alpha + \beta + 1)}{2(s+1)(s+\alpha+\beta+1)(2s+\alpha+\beta)},$$
$$C_s = \frac{(s+\alpha)(s+\beta)(2s+\alpha+\beta+2)}{(s+1)(s+\alpha+\beta+1)(2s+\alpha+\beta)}.$$

Shifted Jacobi polynomials are orthogonal with respect to the weight function

$$w^{(\alpha,\beta)}(x) = (1 - \zeta(x))^{\alpha} (1 + \zeta(x))^{\beta}$$

on $[0, \ell]$. The orthogonality relation is given by the following:

$$(\psi_s(x), \psi_l(x))_w = \int_0^{\ell} \psi_s(x)\psi_l(x)w^{(\alpha,\beta)}(x)\, dx = h_s^{(\alpha,\beta)}\delta_{sl}, \tag{3.3}$$

where the normalization constant $h_s^{(\alpha,\beta)}$ is defined as

$$h_s^{(\alpha,\beta)} = \frac{\ell 2^{\alpha+\beta}\Gamma(s+\alpha+1)\Gamma(s+\beta+1)}{(2s+\alpha+\beta+1)\Gamma(s+1)\Gamma(s+\alpha+\beta+1)}. \tag{3.4}$$

Let $\mathcal{P}_{\aleph}[0, \ell]$ denote the space of polynomials of degree at most $\aleph$. The JGL quadrature rule satisfies the following

$$\int_0^{\ell} \phi(x)w^{(\alpha,\beta)}(x)\, dx = \sum_{j=0}^{\aleph} \varpi_{\aleph,j}^{(\alpha,\beta)}\phi(x_{\aleph,j}), \tag{3.5}$$

with

$$\hat{v}_s(t) \approx \frac{1}{h_s^{(\alpha,\beta)}} \sum_{j=0}^{\aleph} \psi_s(x_{\aleph,j})\varpi_{\aleph,j}^{(\alpha,\beta)} v(x_{\aleph,j}, t) \tag{3.6}$$

notes and weights. The shifted Jacobi-Gauss-Lobatto (SJGL) nodes $\{x_{\aleph,j}\}_{j=0}^{N}$ and weights $\{\varpi_{\aleph,j}^{(\alpha,\beta)}\}_{j=0}^{\aleph}$ on the interval $[0, \ell]$ are given by the following

$$x_{\aleph,j} = \frac{\ell}{2}\left(1 + \zeta_j\right), \quad j = 0, 1, \ldots, \aleph,$$

where $\{\zeta_j\}_{j=0}^{\aleph}$ are the roots of the polynomial $(1 - \zeta^2)\frac{d}{d\zeta}\mathcal{J}_{\aleph}^{(\alpha,\beta)}(\zeta)$. The corresponding weights are defined as follows:

$$\varpi_{\aleph,j}^{(\alpha,\beta)} = \frac{\ell}{2} w_{\aleph,j}^{(\alpha,\beta)}.$$

The spatial tempered-fractional derivatives are approximated using Jacobi differentiation matrices. For $x_{\aleph,n}$ $(n = 1, \ldots, \aleph - 1)$,

$${}_0D_x^{\mu,\gamma} v(x,t) \approx \sum_{i=0}^{\aleph} \left(\sum_{j=0}^{\aleph} \frac{1}{h_j^{(\alpha,\beta)}} \psi_j(x_{\aleph,i})\varpi_{\aleph,i}^{(\alpha,\beta)} {}_0D_x^{\mu,\gamma}\left[\psi_j(x)\right] \right) v(x_{\aleph,i}, t), \tag{3.7}$$

$${}_xD_{\ell}^{\mu,\gamma} v(x,t) \approx \sum_{i=0}^{\aleph} \left(\sum_{j=0}^{\aleph} \frac{1}{h_j^{(\alpha,\beta)}} \psi_j(x_{\aleph,i})\varpi_{\aleph,i}^{(\alpha,\beta)} {}_xD_{\ell}^{\mu,\gamma}\left[\psi_j(x)\right] \right) v(x_{\aleph,i}, t). \tag{3.8}$$

At the nodes $x_{\aleph,n}$ $(n = 1, 2, \ldots, \aleph - 1)$, we have the following

$$ {}_0D_x^{\mu,\gamma} v(x_{\aleph,n}, t) \approx \sum_{i=0}^{\aleph} {}_L D_i^n v(x_{\aleph,i}, t), \tag{3.9} $$

$$ {}_xD_\ell^{\mu,\gamma} v(x_{\aleph,n}, t) \approx \sum_{i=0}^{\aleph} {}_R D_i^n v(x_{\aleph,i}, t), \tag{3.10} $$

where

$$ {}_L D_i^n = \sum_{j=0}^{\aleph} \frac{1}{h_j^{(\alpha,\beta)}} \psi_j(x_{\aleph,i}) \varpi_{\aleph,i}^{(\alpha,\beta)} {}_0D_{x_{\aleph,n}}^{\mu,\gamma} \left[\psi_j(x_{\aleph,n})\right], \tag{3.11} $$

$$ {}_R D_i^n = \sum_{j=0}^{\aleph} \frac{1}{h_j^{(\alpha,\beta)}} \psi_j(x_{\aleph,i}) \varpi_{\aleph,i}^{(\alpha,\beta)} {}_{x_{\aleph,n}}D_\ell^{\mu,\gamma} \left[\psi_j(x_{\aleph,n})\right]. \tag{3.12} $$

The tempered fractional diffusion derivative's spectral discretization can be represented in a compact notation as follows:

$$ \partial_{|x|}^{\mu,\gamma} v(x_{\aleph,n}, t) \approx \sum_{i=0}^{\aleph} \mathfrak{D}_i^n v(x_{\aleph,i}, t) + \frac{\gamma^\mu}{\cos\left(\frac{\mu\pi}{2}\right)} v(x_{\aleph,n}, t), \tag{3.13} $$

where

$$ \mathfrak{D}_i^n = -\frac{1}{2\cos\left(\frac{\mu\pi}{2}\right)} \left({}_L D_i^n + {}_R D_i^n\right). \tag{3.14} $$

Let us denote the following

$$ v_n(t) = v(x_{\aleph,n}, t), \quad p_n(t) = p(x_{\aleph,n}, t). $$

As a result of these manipulations, we arrive at the following system of semi-discrete equations in the time direction

$$ \dot{v}_n(t) = \epsilon \sum_{i=0}^{\aleph} \mathfrak{D}_i^n(t) v_i(t) + \frac{\epsilon\gamma^\mu}{\cos\left(\frac{\mu\pi}{2}\right)} v_n(t) + p_n(t) + v_n(t) - v_n^3(t). \tag{3.15} $$

The boundary conditions are imposed exactly as $v_0(t) = v_\aleph(t) = 0$.

4. Two-dimensional spectral discretization

In this section, we extend the one-dimensional spectral discretization scheme to solve the following two-dimensional tempered-fractional Allen-Cahn equation:

$$ \frac{\partial v}{\partial t}(x, y, t) - \epsilon\, \partial_{|x|}^{\mu,\gamma} v(x, y, t) - \epsilon\, \partial_{|y|}^{\mu,\gamma} v(x, y, t) = v(x, y, t) - v^3(x, y, t) + p(x, y, t), \tag{4.1} $$

where $(x, y) \in \Omega = (0, \ell_x) \times (0, \ell_y)$, and $t \in I = (0, T]$. The boundary and initial conditions are given by the following:

$$ v(0, y, t) = v(\ell_x, y, t) = v(x, 0, t) = v(x, \ell_y, t) = 0, \quad \text{for } t \in I, \text{ on } \partial\Omega, $$

$$v(x, y, 0) = g(x, y), \quad \text{on } \Omega,$$

where $1 < \mu < 2$ and $\gamma > 0$.

The solution $v(x, y, t)$ is expressed in terms of unknown variable coefficients $\hat{v}_{s,r}(t)$ as follows:

$$v(x, y, t) \approx \sum_{s=0}^{\aleph_x} \sum_{r=0}^{\aleph_y} \hat{v}_{s,r}(t)\psi_s(x)\phi_r(y),$$

where $\psi_s(x)$ and $\phi_r(y)$ are shifted Jacobi polynomials defined on the physical domains $[0, \ell_x]$ and $[0, \ell_y]$, respectively. These basis functions are constructed from the standard Jacobi polynomials $\mathcal{J}_s^{(\alpha,\beta)}(\zeta)$ and $\mathcal{J}_r^{(\alpha,\beta)}(\eta)$ defined on $[-1, 1]$ via the following transformations:

$$\psi_s(x) = \mathcal{J}_s^{(\alpha,\beta)}(\zeta(x)), \quad \text{where } \zeta(x) = \frac{2x}{\ell_x} - 1,$$

$$\phi_r(y) = \mathcal{J}_r^{(\alpha,\beta)}(\eta(y)), \quad \text{where } \eta(y) = \frac{2y}{\ell_y} - 1.$$

These bases are orthogonal with respect to the weight functions $w^{(\alpha,\beta)}(x)$ and $w^{(\alpha,\beta)}(y)$ on $[0, \ell_x]$ and $[0, \ell_y]$, respectively. The orthogonality relations are given by the following:

$$(\psi_s(x), \psi_l(x))_w = \int_0^{\ell_x} \psi_s(x)\psi_l(x)w^{(\alpha,\beta)}(x)\,dx = h_s^{(\alpha,\beta)}\delta_{sl},$$

$$(\phi_r(y), \phi_k(y))_w = \int_0^{\ell_y} \phi_r(y)\phi_k(y)w^{(\alpha,\beta)}(y)\,dy = h_r^{(\alpha,\beta)}\delta_{rk}.$$

The normalization constants $h_{x,s}^{(\alpha,\beta)}$ and $h_{y,r}^{(\alpha,\beta)}$ for the shifted Jacobi polynomials $\psi_s(x)$ and $\psi_r(y)$ are given by the following:

$$h_{x,s}^{(\alpha,\beta)} = \frac{\ell_x\, 2^{\alpha+\beta}\Gamma(s+\alpha+1)\Gamma(s+\beta+1)}{(2s+\alpha+\beta+1)\Gamma(s+1)\Gamma(s+\alpha+\beta+1)},$$

$$h_{y,r}^{(\alpha,\beta)} = \frac{\ell_y\, 2^{\alpha+\beta}\Gamma(r+\alpha+1)\Gamma(r+\beta+1)}{(2r+\alpha+\beta+1)\Gamma(r+1)\Gamma(r+\alpha+\beta+1)}.$$

The JGL quadrature rule is applied in both spatial directions as follows:

$$\int_0^{\ell_x}\int_0^{\ell_y} \phi(x, y)w^{(\alpha,\beta)}(x)w^{(\alpha,\beta)}(y)\,dx\,dy \approx \sum_{i=0}^{\aleph_x}\sum_{j=0}^{\aleph_y} \varpi_{\aleph_x,i}^{(\alpha,\beta)}\varpi_{\aleph_y,j}^{(\alpha,\beta)}\phi(x_{\aleph_x,i}, y_{\aleph_y,j}).$$

The JGL nodes and weights in the x-direction are given by the following

$$x_{\aleph_x,i} = \frac{\ell_x}{2}(1 + \zeta_i), \quad i = 0, 1, \ldots, \aleph_x, \quad \varpi_{\aleph_x,j}^{(\alpha,\beta)} = \frac{\ell_x}{2}w_{\aleph,j}^{(\alpha,\beta)}.$$

Similarly, the JGL nodes and weights in the y-direction are given by the following

$$y_{\aleph_y,j} = \frac{\ell_y}{2}\left(1 + \eta_j\right), \quad j = 0, 1, \ldots, \aleph_y, \quad \varpi_{\aleph_y,j}^{(\alpha,\beta)} = \frac{\ell_y}{2}w_{\aleph,j}^{(\alpha,\beta)}.$$

The spatial tempered-fractional and integer-order derivatives are approximated using Jacobi differentiation matrices in both x and y directions, for $x_{\aleph_x,n}$ and $y_{\aleph_y,m}$.

The coefficients $\hat{v}_{s,r}(t)$ are computed via the discrete inner product as follows:

$$\hat{v}_{s,r}(t) \approx \frac{1}{h_s^{(\alpha,\beta)} h_r^{(\alpha,\beta)}} \sum_{j=0}^{\aleph_x} \sum_{k=0}^{\aleph_y} \psi_s(x_{\aleph_x,j}) \phi_r(y_{\aleph_y,k}) \varpi_{\aleph_x,j}^{(\alpha,\beta)} \varpi_{\aleph_y,k}^{(\alpha,\beta)} v(x_{\aleph_x,j}, y_{\aleph_y,k}, t). \tag{4.2}$$

For $x_{\aleph_x,n}$ ($n = 1, \ldots, \aleph_x - 1$) and $y_{\aleph_y,m}$ ($m = 1, \ldots, \aleph_y - 1$),

$$\begin{aligned} {}_0D_x^{\mu,\gamma} v(x,y,t) \approx \sum_{i=0}^{\aleph_x} \sum_{j=0}^{\aleph_y} \Bigg(& \sum_{k=0}^{\aleph_x} \sum_{l=0}^{\aleph_y} \frac{1}{h_k^{(\alpha,\beta)} h_l^{(\alpha,\beta)}} \psi_k(x_{\aleph_x,i}) \phi_l(y_{\aleph_y,j}) \\ & \times \varpi_{\aleph_x,i}^{(\alpha,\beta)} \varpi_{\aleph_y,j}^{(\alpha,\beta)} {}_0D_x^{\mu,\gamma} \left[\psi_k(x)\right] \phi_l(y) \Bigg) v(x_{\aleph_x,i}, y_{\aleph_y,j}, t), \end{aligned} \tag{4.3}$$

$$\begin{aligned} {}_xD_{\ell_x}^{\mu,\gamma} v(x,y,t) \approx \sum_{i=0}^{\aleph_x} \sum_{j=0}^{\aleph_y} \Bigg(& \sum_{k=0}^{\aleph_x} \sum_{l=0}^{\aleph_y} \frac{1}{h_k^{(\alpha,\beta)} h_l^{(\alpha,\beta)}} \psi_k(x_{\aleph_x,i}) \phi_l(y_{\aleph_y,j}) \\ & \times \varpi_{\aleph_x,i}^{(\alpha,\beta)} \varpi_{\aleph_y,j}^{(\alpha,\beta)} {}_xD_{\ell_x}^{\mu,\gamma} \left[\psi_k(x)\right] \phi_l(y) \Bigg) v(x_{\aleph_x,i}, y_{\aleph_y,j}, t). \end{aligned} \tag{4.4}$$

At the nodes $x_{\aleph_x,n}$ ($n = 1, \ldots, \aleph_x - 1$) and $y_{\aleph_y,m}$ ($m = 1, \ldots, \aleph_y - 1$), we have the following

$${}_0D_x^{\mu,\gamma} v(x_{\aleph_x,n}, y_{\aleph_y,m}, t) \approx \sum_{i=0}^{\aleph_x} \sum_{j=0}^{\aleph_y} {}_LD_{i,j}^{n,m} v(x_{\aleph_x,i}, y_{\aleph_y,j}, t), \tag{4.5}$$

$${}_0D_y^{\mu,\gamma} v(x_{\aleph_x,n}, y_{\aleph_y,m}, t) \approx \sum_{i=0}^{\aleph_x} \sum_{j=0}^{\aleph_y} {}_L\overline{D}_{i,j}^{n,m} v(x_{\aleph_x,i}, y_{\aleph_y,j}, t), \tag{4.6}$$

$${}_xD_{\ell_x}^{\mu,\gamma} v(x_{\aleph_x,n}, y_{\aleph_y,m}, t) \approx \sum_{i=0}^{\aleph_x} \sum_{j=0}^{\aleph_y} {}_RD_{i,j}^{n,m} v(x_{\aleph_x,i}, y_{\aleph_y,j}, t), \tag{4.7}$$

$${}_yD_{\ell_y}^{\mu,\gamma} v(x_{\aleph_x,n}, y_{\aleph_y,m}, t) \approx \sum_{i=0}^{\aleph_x} \sum_{j=0}^{\aleph_y} {}_R\overline{D}_{i,j}^{n,m} v(x_{\aleph_x,i}, y_{\aleph_y,j}, t), \tag{4.8}$$

where

$${}_LD_{i,j}^{n,m} = \sum_{k=0}^{\aleph_x} \sum_{l=0}^{\aleph_y} \frac{1}{h_k^{(\alpha,\beta)} h_l^{(\alpha,\beta)}} \psi_k(x_{\aleph_x,i}) \phi_l(y_{\aleph_y,j}) \varpi_{\aleph_x,i}^{(\alpha,\beta)} \varpi_{\aleph_y,j}^{(\alpha,\beta)} {}_0D_{x_{\aleph_x,n}}^{\mu,\gamma} \left[\psi_k(x_{\aleph_x,n})\right] \phi_l(y_{\aleph_y,m}), \tag{4.9}$$

$${}_L\overline{D}_{i,j}^{n,m} = \sum_{k=0}^{\aleph_x} \sum_{l=0}^{\aleph_y} \frac{1}{h_k^{(\alpha,\beta)} h_l^{(\alpha,\beta)}} \psi_k(x_{\aleph_x,i}) \phi_l(y_{\aleph_y,j}) \varpi_{\aleph_x,i}^{(\alpha,\beta)} \varpi_{\aleph_y,j}^{(\alpha,\beta)} \psi_k(x_{\aleph_x,n}) {}_0D_{y_{\aleph_y,m}}^{\mu,\gamma} \left[\phi_l(y_{\aleph_y,m})\right], \tag{4.10}$$

$${}_RD_{i,j}^{n,m} = \sum_{k=0}^{\aleph_x} \sum_{l=0}^{\aleph_y} \frac{1}{h_k^{(\alpha,\beta)} h_l^{(\alpha,\beta)}} \psi_k(x_{\aleph_x,i}) \phi_l(y_{\aleph_y,j}) \varpi_{\aleph_x,i}^{(\alpha,\beta)} \varpi_{\aleph_y,j}^{(\alpha,\beta)} {}_{x_{\aleph_x,n}}D_{\ell_x}^{\mu,\gamma} \left[\psi_k(x_{\aleph_x,n})\right] \phi_l(y_{\aleph_y,m}), \tag{4.11}$$

$$ {}_R\overline{D}_{i,j}^{n,m} = \sum_{k=0}^{\aleph_x} \sum_{l=0}^{\aleph_y} \frac{1}{h_k^{(\alpha,\beta)} h_l^{(\alpha,\beta)}} \psi_k(x_{\aleph_x,i}) \phi_l(y_{\aleph_y,j}) \varpi_{\aleph_x,i}^{(\alpha,\beta)} \varpi_{\aleph_y,j}^{(\alpha,\beta)} \psi_k(x_{\aleph_x,n})_{y_{\aleph_y,m}} D_{\ell_y}^{\mu,\gamma} \left[\phi_l(y_{\aleph_y,m})\right]. \tag{4.12} $$

The tempered fractional diffusion derivative's spectral discretization can be represented in a compact notation as follows:

$$ \partial_{|x|}^{\mu,\gamma} v(x_{\aleph_x,n}, y_{\aleph_y,m}, t) \approx \sum_{i=0}^{\aleph_x} \sum_{j=0}^{\aleph_y} \mathfrak{D}_{i,j}^{n,m} v(x_{\aleph_x,i}, y_{\aleph_y,j}, t) + \frac{\gamma^\mu}{\cos\left(\frac{\mu\pi}{2}\right)} v(x_{\aleph_x,n}, y_{\aleph_y,m}, t), \tag{4.13} $$

$$ \partial_{|y|}^{\mu,\gamma} v(x_{\aleph_x,n}, y_{\aleph_y,m}, t) \approx \sum_{i=0}^{\aleph_x} \sum_{j=0}^{\aleph_y} \overline{\mathfrak{D}}_{i,j}^{n,m} v(x_{\aleph_x,i}, y_{\aleph_y,j}, t) + \frac{\gamma^\mu}{\cos\left(\frac{\mu\pi}{2}\right)} v(x_{\aleph_x,n}, y_{\aleph_y,m}, t), \tag{4.14} $$

where

$$ \mathfrak{D}_{i,j}^{n,m} = -\frac{1}{2\cos\left(\frac{\mu\pi}{2}\right)} \left({}_L D_{i,j}^{n,m} + {}_R D_{i,j}^{n,m}\right), \tag{4.15} $$

$$ \overline{\mathfrak{D}}_{i,j}^{n,m} = -\frac{1}{2\cos\left(\frac{\mu\pi}{2}\right)} \left({}_L \overline{D}_{i,j}^{n,m} + {}_R \overline{D}_{i,j}^{n,m}\right). \tag{4.16} $$

Let us denote the following

$$ \begin{aligned} v_{n,m}(t) &= v(x_{\aleph_x,n}, y_{\aleph_y,m}, t), \\ p_{n,m}(t) &= p(x_{\aleph_x,n}, y_{\aleph_y,m}, t). \\ g_{n,m}(t) &= g(x_{\aleph_x,n}, y_{\aleph_y,m}, t). \end{aligned} $$

As a result of these manipulations, we arrive at the following system of semi-discrete equations in the time direction

$$ \begin{aligned} \dot{v}_{n,m}(t) = \epsilon \sum_{i=1}^{\aleph_x-1} \sum_{j=1}^{\aleph_y-1} \mathfrak{D}_{i,j}^{n,m} v_{i,j}(t) + \epsilon \sum_{i=1}^{\aleph_x-1} \sum_{j=1}^{\aleph_y-1} \overline{\mathfrak{D}}_{i,j}^{n,m} v_{i,j}(t) \\ + \frac{2\epsilon\gamma^\mu}{\cos\left(\frac{\mu\pi}{2}\right)} v_{n,m}(t) + p_{n,m}(t) + v_{n,m}(t) - v_{n,m}^3(t), \end{aligned} \tag{4.17} $$

with the initial condition $v_{n,m}(0) = g_{n,m}$. In fact, this allows for the exact imposition of boundary conditions as follows: $v_{0,k}(t) = v_{\aleph_x,k}(t) = v_{j,0}(t) = v_{j,\aleph_y}(t) = 0$.

5. Implicit Runge-Kutta method

To numerically solve the provided system of differential equations, we utilize an IRK approach, which The system is expressed as follows:

$$ \frac{du_j}{dt} = F_j(t, u_1, \ldots, u_{N-1}), \quad j = 1, \ldots, N-1, \quad t \in (0, 1], \tag{5.1} $$

where the initial conditions are

$$u_j(0) = h_j, \quad j = 1, \ldots, N-1. \tag{5.2}$$

We approximate the solution using an IRK technique. For a fixed time step size Δt, the discrete time points are defined as follows: $t_n = t_0 + n\Delta t, \quad n = 0, 1, 2, \ldots$, where $u_j^{(n)}$ represents the numerical approximation of the exact solution $u_j(t_n)$.

The IRK method iteratively updates the solution as follows:

$$u_j^{(n+1)} = u_j^{(n)} + \Delta t \sum_{s=1}^{p} d_s \ell_{j,s}^{(n)}, \quad j = 1, \ldots, N-1. \tag{5.3}$$

Here, the stage values $\ell_{j,s}^{(n)}$ are determined by the following system:

$$\ell_{j,s}^{(n)} = F_j\left(t_n + e_s\Delta t, R_{j,s}^{(n)}\right), \quad s = 1, \ldots, p. \tag{5.4}$$

The intermediate approximations $R_{j,s}^{(n)}$ are computed as follows:

$$R_{j,s}^{(n)} = u_j^{(n)} + \Delta t \sum_{r=1}^{p} f_{s,r} \ell_{j,r}^{(n)}, \quad s = 1, \ldots, p. \tag{5.5}$$

In this formulation, Δt denotes the step size, and the coefficients $f_{s,r}$, d_s, and e_s characterize the Runge-Kutta method. Table 1 organizes these coefficients into a Butcher tableau.

Table 1. Butcher tableau for the implicit Runge-Kutta method.

e_1	f_{11}	$\ldots$	f_{1p}
$\vdots$	$\vdots$	$\ddots$	$\vdots$
e_p	f_{p1}	$\ldots$	f_{pp}
	d_1	$\ldots$	d_p

6. Numerical results

Example 1. *In this example, we consider the following Allen-Cahn equation in a tempered fractional one-dimensional form with* $\epsilon = 0.1$*:*

$$\frac{\partial v}{\partial t}(x,t) - 0.1\, \partial_{|x|}^{\mu,\gamma} v(x,t) = v(x,t) - v^3(x,t) + p(x,t), \quad \text{in } \Omega = (0,1), \text{ for } I = (0,T]. \tag{6.1}$$

The boundary and initial conditions are given by the following:

$$v(0,t) = v(1,t) = 0, \quad \text{for } t \in I, \text{ on } \partial\Omega,$$

$$v(x,0) = x^3(1-x)^3, \quad \text{on } \Omega.$$

The tempered-fractional Allen-Cahn equation admits an exact solution $v(x,t) = e^{-t}x^3(1-x)^3$.

Recently, Zhang et al. [28] presented and analyzed high-order implicit-explicit Runge-Kutta schemes to solve the space-fractional Allen-Cahn equation, thus ensuring high-order convergence through spatial discretization with a second-order fractional centered difference method and numerical validation. To validate the superior accuracy of the proposed method over the approach in [28], we conduct a systematic comparison under identical computational settings:

- Without tempering ($\gamma = 0$),
- Fractional orders $\mu = 1.2$ and $\mu = 1.8$, and
- Terminal time $T = 4$.

Table 2 presents the maximum absolute errors for both methods at varying spatial resolutions (N) with the Jacobi parameters $\alpha = 2, \beta = 2$. The results demonstrate that our method achieves significantly smaller errors across all tested grid sizes compared to [28].

Table 2. Maximum absolute errors of Example 1 with $\gamma = 0$, $\alpha = 2\beta = 2$ and $T = 4$.

μ	N	Present method	N	Method [28]
1.2	7	2.498×10^{-16}	16	5.906×10^{-4}
	8	2.183×10^{-16}	32	1.523×10^{-4}
	9	2.400×10^{-16}	64	3.832×10^{-5}
	10	2.421×10^{-16}	128	9.627×10^{-6}
1.8	7	4.510×10^{-17}	16	1.139×10^{-3}
	8	4.163×10^{-17}	32	2.597×10^{-4}
	9	5.106×10^{-17}	64	6.320×10^{-5}
	10	6.071×10^{-17}	128	1.564×10^{-5}

We consider the following three cases to display the accuracy of the proposed method:

- Case 1: without Tempering ($\gamma = 0$):
  For $\gamma = 0$, $\mu = 1.2$, $\alpha = 2$, $\beta = 1$, and $N = 11$, Figures 1–3 illustrate the approximate solution, absolute errors, and comparison to the exact solution, respectively. The maximum absolute error demonstrates excellent agreement with the analytical solution. The temporal and spatial error profiles in Figure 2 further confirm a uniform error distribution.
  To increase the fractional order to $\mu = 1.8$ (Figures 4–6), the proposed method maintains high-order accuracy, thus highlighting its robustness to variations in μ.
- Case 2: with tempering ($\gamma = 1$):
  For ($\gamma = 1$, $\mu = 1.2$, $\alpha = 2$, $\beta = 4$, $N = 11$), Figures 7–9 illustrate the approximate solution, absolute errors, and comparison to the exact solution, respectively. The maximum absolute error demonstrates excellent agreement with the analytical solution.
  For $\mu = 1.8$ with tempering (Figures 10–12), the method retains high-order accuracy, even under steeper spatial gradients. The side-by-side plots in Figure 12 confirm that the numerical solution closely aligns with the exact profile, thus validating the scheme's adaptability to tempered fractional operators.

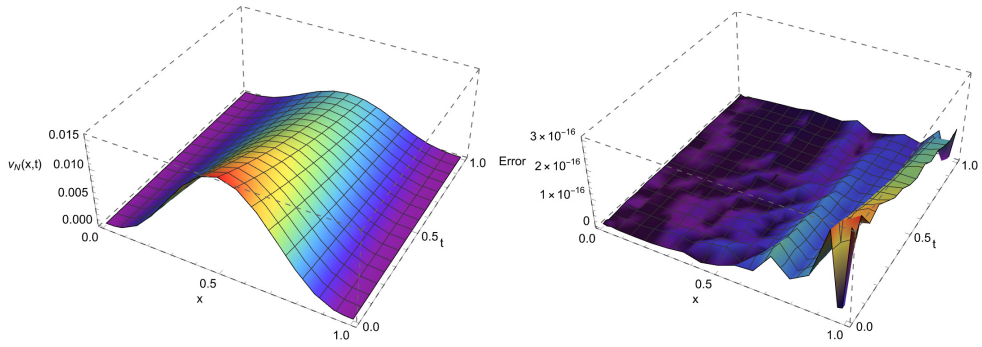

Figure 1. The approximate solution and the absolute error function for Example 1 with $\gamma = 0$, $\mu = 1.2$, $T = 1$, $\alpha = 2\beta = 1$, and $N = 11$.

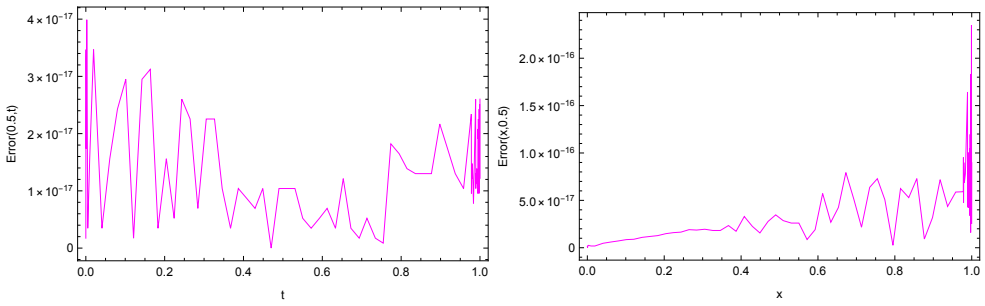

Figure 2. The absolute error function for Example 1 with $\gamma = 0$, $\mu = 1.2$, $T = 1$, $\alpha = 2\beta = 1$, and $N = 11$.

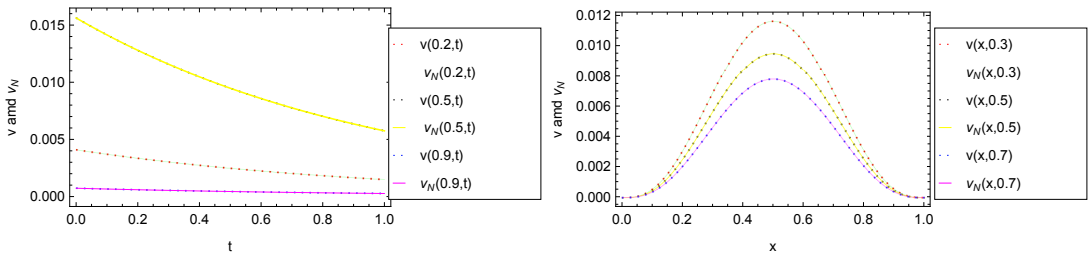

Figure 3. The approximate and the exact solutions for Example 1 with $\gamma = 0$, $\mu = 1.2$, $T = 1$, $\alpha = 2\beta = 1$, and $N = 11$.

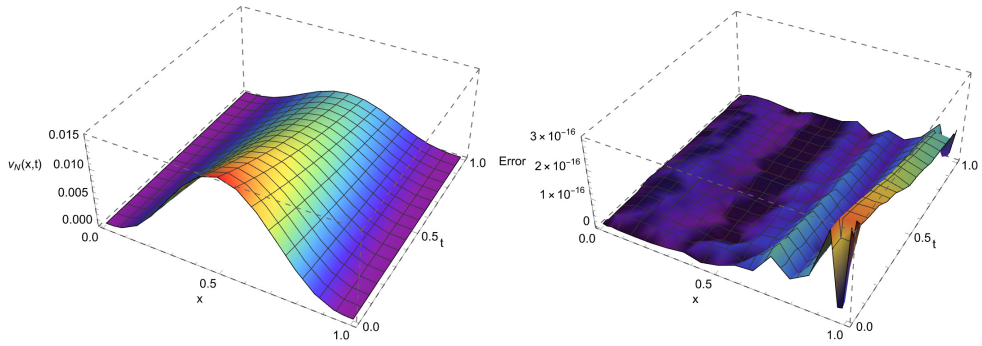

Figure 4. The approximate solution and the absolute error function for Example 1 with $\gamma = 0$, $\mu = 1.8$, $T = 1$, $\alpha = 2\beta = 1$, and $N = 11$.

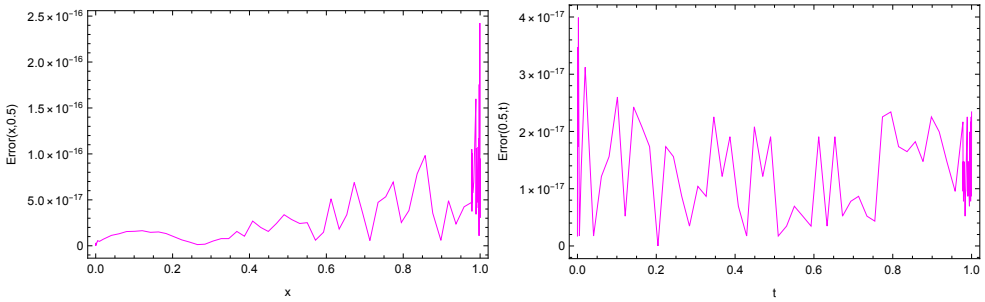

Figure 5. The absolute error function for Example 1 with $\gamma = 0$, $\mu = 1.8$, $T = 1$, $\alpha = 2\beta = 1$, and $N = 11$.

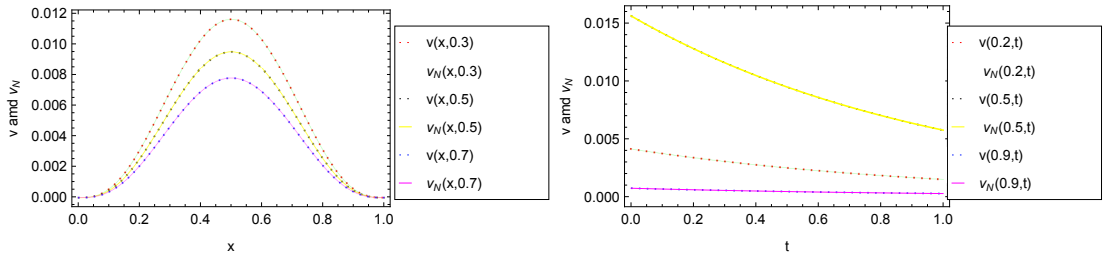

Figure 6. The approximate and the exact solutions for Example 1 with $\gamma = 0$, $\mu = 1.8$, $T = 1$, $\alpha = 2\beta = 1$, and $N = 11$.

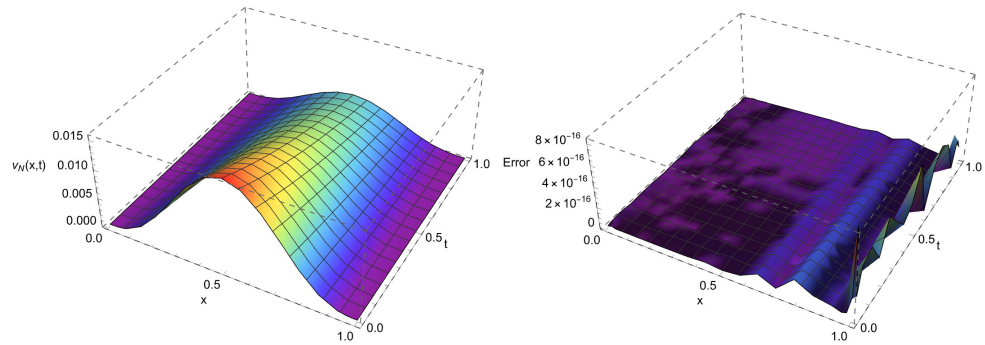

Figure 7. The approximate solution and the absolute error function for Example 1 with $\gamma = 1$, $\mu = 1.2$, $T = 1$, $\alpha = 2\beta = 4$, and $N = 11$.

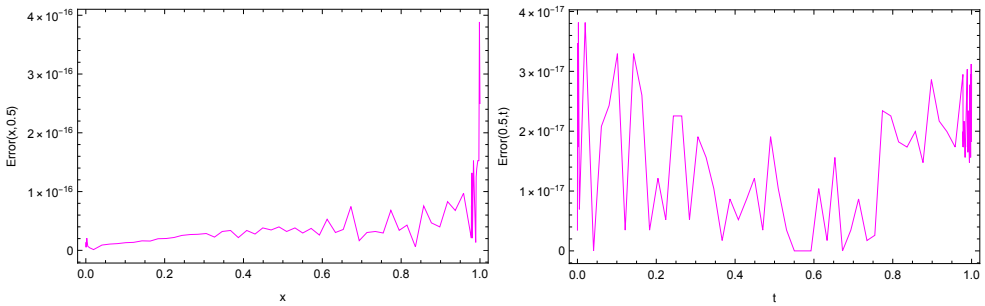

Figure 8. The absolute error function for Example 1 with $\gamma = 1$, $\mu = 1.2$, $T = 1$, $\alpha = 2\beta = 4$, and $N = 11$.

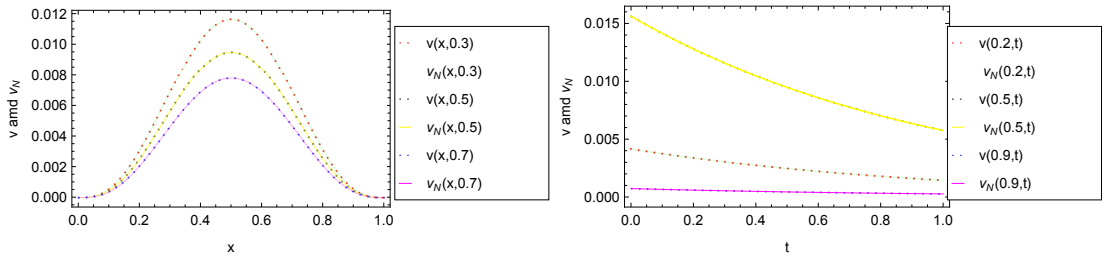

Figure 9. The approximate and the exact solutions for Example 1 with $\gamma = 1$, $\mu = 1.2$, $T = 1$, $\alpha = 2\beta = 4$, and $N = 11$.

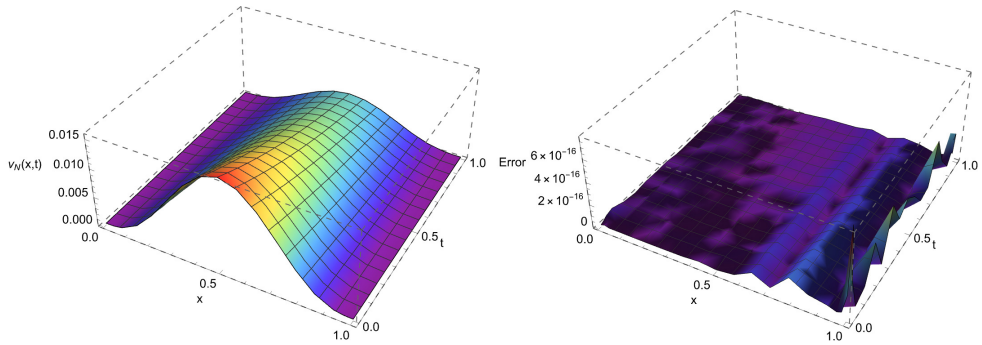

Figure 10. The approximate solution and the absolute error function for Example 1 with $\gamma = 1$, $\mu = 1.8$, $T = 1$, $\alpha = 2\beta = 4$, and $N = 11$.

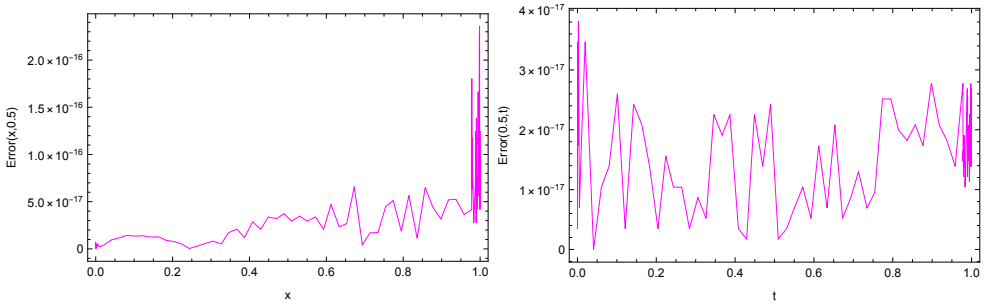

Figure 11. The absolute error function for Example 1 with $\gamma = 1$, $\mu = 1.8$, $T = 1$, $\alpha = 2\beta = 4$, and $N = 11$.

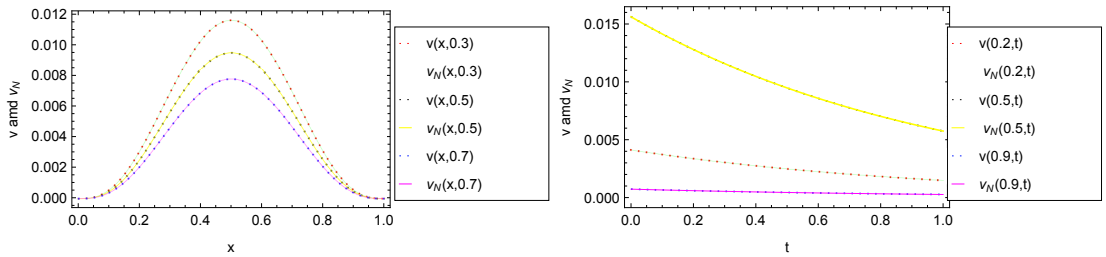

Figure 12. The approximate and the exact solutions for Example 1 with $\gamma = 1$, $\mu = 1.8$, $T = 1$, $\alpha = 2\beta = 4$, and $N = 11$.

Example 2. *In this example, we consider the following two-dimensional tempered-fractional Allen-Cahn equation on the domain* $\Omega = [0,1] \times [0,1]$ *with* $\epsilon = 0.1$*:*

$$\frac{\partial v}{\partial t}(x,y,t) - \epsilon\, \partial^{\mu,\gamma}_{|x|} v(x,y,t) - \epsilon\, \partial^{\mu,\gamma}_{|y|} v(x,y,t) = v(x,y,t) - v^3(x,y,t) + p(x,y,t). \tag{6.2}$$

The boundary and initial conditions are given by the following

$$v(0,y,t) = v(\ell_x,y,t) = v(x,0,t) = v(x,\ell_y,t) = 0, \quad \text{for } t \in (0,1], \text{ on } \partial\Omega,$$

$$v(x,y,0) = x^3y^3(1-x)^3(1-y)^3, \quad \text{on } \Omega.$$

The tempered-fractional Allen-Cahn equation admits the exact solution

$$v(x,t) = e^{-t}x^3(1-x)^3y^3(1-y)^3.$$

We consider the following three characteristic cases to demonstrate the high-order accuracy and tempering sensitivity of the proposed method:

- Negative tempering ($\gamma = -1$): in Figure 13, the proposed method evaluates the space-fractional problem under negative tempering with fractional orders $\mu = 1.2$, 1.6, and 1.8, the Jacobi parameters $\alpha = 2\beta = 2$, and spatial resolution $N = 15$, thus demonstrating high accuracy.
- Without tempering ($\gamma = 0$): in Figure 14, the scheme maintains high-accuracy across the same range and parameters μ.
- Positive tempering ($\gamma = 1$): in Figure 15, the method achieves superior accuracy for all tested μ values, thus underscoring its adaptability to tempered fractional operators.

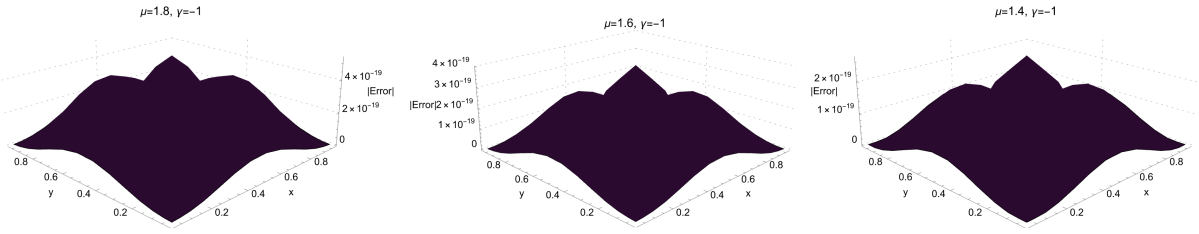

Figure 13. The absolute error function of the approximate solution of Example 2 with the tempering parameter $\gamma = -1$, and with $\alpha = 2\beta = 2$, $N = 15$ and various fractional orders $\mu = 1.4$, 1.6, and 1.8.

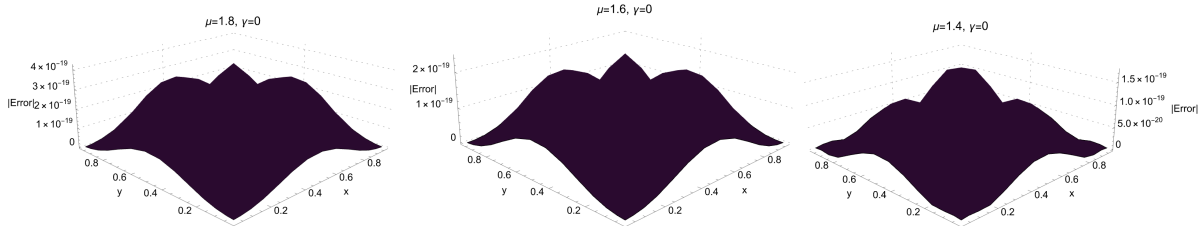

Figure 14. The absolute error function of the approximate solution of Example 2 with the tempering parameter $\gamma = 0$ and with $\alpha = 2\beta = 2$, $N = 15$, and various fractional orders $\mu = 1.4$, 1.6, and 1.8.

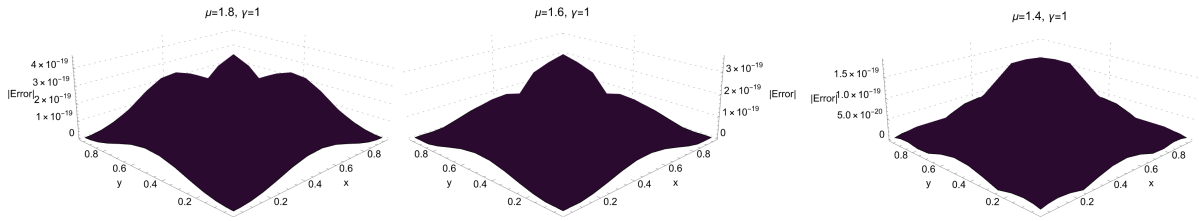

Figure 15. The absolute error function of the approximate solution of Example 2 with the tempering parameter $\gamma = 1$ and with $\alpha = 2\beta = 2$, $N = 15$, and various fractional orders $\mu = 1.4$, 1.6, and 1.8.

7. Conclusions

This paper presented a high-order spectral collocation method to solve tempered fractional Allen-Cahn equations in one and two dimensions. The method's ability to incorporate exponential tempering enables precise modeling of systems with truncated long-range interactions. Numerical experiments demonstrated superior accuracy over existing methods. The extension to 2D via tensor product bases highlights its scalability, while exact boundary enforcement ensures robustness in complex geometries. Looking ahead, future research will explore several important directions, including a rigorous analysis of the scheme's energy stability properties and the development of structure-preserving temporal discretizations for long-term simulations. Additionally, we will investigate extensions to 3D problems, adaptive mesh refinement techniques, and applications in diverse fields such as combustion and financial modeling. This approach bridges the gap between spectral methods and tempered fractional partial differential equation (PDEs), offering a powerful tool to explore non-local dynamics in scientific and engineering contexts.

Author contributions

Maged Z. Youssef, Mahmoud A. Zaky, Faizah A.H. Alomari, Amra Al Kenany, Samer Ezz-Eldien: Conceptualization, Formal analysis, Methodology, Writing-original draft, Writing-review & editing. All authors of this article have been contributed equally. All authors have read and approved the final version of the manuscript for publication.

Use of Generative-AI tools declaration

The authors declare that they have not used Artificial Intelligence (AI) tools in the creation of this article.

Acknowledgments

This work was supported and funded by the Deanship of Scientific Research at Imam Mohammad Ibn Saud Islamic University (IMSIU) (grant number IMSIU-DDRSP2502).

Funding

This work was supported and funded by the Deanship of Scientific Research at Imam Mohammad Ibn Saud Islamic University (IMSIU) (grant number IMSIU-DDRSP2502).

Conflict of interest

The authors declare that they have no conflicts of interest.

References

1. S. M. Allen, J. W. Cahn, A microscopic theory for antiphase boundary motion and its application to antiphase domain coarsening, *Acta Metall.*, **27** (1979), 1085–1095. https://doi.org/10.1016/0001-6160(79)90196-2
2. A. A. Wheeler, M. J. Boettinger, G. B. Mcfadden, Phase-field model for isothermal phase transitions in binary alloys, *Phys. Rev. A*, **45** (1992), 7424–7439. https://doi.org/10.1103/PhysRevA.45.7424
3. L. Golubovic, A. Levandovsky, D. Moldovan, Interface dynamics and far-from-equilibrium phase transitions in multilayer epitaxial growth and erosion on crystal surfaces: continuum theory insights, *East Asian J. Appl. Math.*, **1** (2011), 297–371. https://doi.org/10.4208/eajam.040411.030611a
4. J. Kim, Phase field models for multi-component fuid flows, *Commun. Comput. Phys.*, **12** (2012), 613–661. https://doi.org/10.4208/cicp.301110.040811a
5. Y. Yu, W Zhou, Z. Zhang, Q. Bi, Analysis on the motion of nonlinear vibration with fractional order and time variable mass, *Appl. Math. Lett.*, **124** (2022), 107621. https://doi.org/10.1016/j.aml.2021.107621
6. B. Yin, Y. Liu, H. Li, S. He, Fast algorithm based on TT-M FE system for space fractional Allen-Cahn equations with smooth and non-smooth solutions, *J. Comput. Phys.*, **379** (2019), 351–372. https://doi.org/10.1016/j.jcp.2018.12.004
7. H. Li, Y. Li, Y. Zeng, Z. Luo, A reduced-dimension extrapolation two-grid Crank-Nicolson finite element method of unknown solution coefficient vectors for spatial fractional nonlinear Allen-Cahn equations, *Comput. Math. Appl.*, **167** (2024), 110–122. https://doi.org/10.1016/j.camwa.2024.05.007
8. H. Yuan, Z. Hui, A class of higher-order time-splitting Monte Carlo method for fractional Allen-Cahn equation, *Appl. Math. Lett.*, **163** (2025), 109467. https://doi.org/10.1016/j.aml.2025.109467
9. L. Bu, L. Mei, Y. Hou, Stable second-order schemes for the space-fractional Cahn-Hilliard and Allen-Cahn equations, *Comput. Math. Appl.*, **78** (2019), 3485–3500. https://doi.org/10.1016/j.camwa.2019.08.015
10. B. Zhang, Y. Yang, An adaptive unconditional maximum principle preserving and energy stability scheme for the space fractional Allen-Cahn equation, *Comput. Math. Appl.*, **139** (2023), 28–37. https://doi.org/10.1016/j.camwa.2023.02.022

11. S. Zhai, C. Ye, Z. Weng, A fast and efficient numerical algorithm for fractional Allen-Cahn with precise nonlocal mass conservation, *Appl. Math. Lett.*, **103** (2020), 106190. https://doi.org/10.1016/j.aml.2019.106190

12. W. Chen, D. Lu, H. Chen, H. Liu, Crank-Nicolson Legendre spectral approximation for space-fractional Allen-Cahn equation, *Elect. J. Differ. Equ. Texas State Uni.*, **2019** (2019), 76. https://doi.org/10.37218/ejde.2019.76.1

13. T. Hou, T. Tang, J. Yang, Numerical analysis of fully discretized Crank-Nicolson scheme for fractional-in-space Allen-Cahn equations, *J. Sci. Comput.*, **72** (2017), 1214–1231. https://doi.org/10.1007/s10915-017-0396-9

14. B. Zhang, Y. Yang, A new linearized maximum principle preserving and energy stability scheme for the space fractional Allen-Cahn equation, *Numer. Algor.*, **93** (2023), 179–202. https://doi.org/10.1007/s11075-022-01411-x

15. M. M. Meerschaert, F. Sabzikar, M. S. Phanikumar, A. Zeleke, Tempered fractional timeseries model for turbulence in geophysical flows, *J. Stat. Mech.: Theory Exper.*, **14** (2014), 1742–5468. https://doi.org/10.1088/1742-5468/2014/09/P09023

16. M. M. Meerschaert, Y. Zhang, B. Baeumer, Tempered anomalous diffusion in heteroge-neous systems, *Geophys. Res. Lett.*, **35** (2008), L17403. https://doi.org/10.1029/2008GL034899

17. A. Cartea, D. Del-Castillo-Negrete, Fractional diffusion models of option prices in marketswith jumps, *Phys. A: Stat. Mech. Appl.*, **374** (2007), 749–763. https://doi.org/10.1016/j.physa.2006.08.071

18. A. Hanyga, Wave propagation in media with singular memory, *Math. Comput. Model.*, **34** (2001), 1399–1421. https://doi.org/https://doi.org/10.1016/S0895-7177(01)00137-6

19. M. A. Zaky, Existence, uniqueness and numerical analysis of solutions of tempered fractional boundary value problems, *Appl. Numer. Math.*, **145** (2019), 429–457. https://doi.org/10.1016/j.apnum.2019.05.008

20. R. Almeida, N. Martins, J. V. C. Sousa, Fractional tempered differential equations depending on arbitrary kernels, *AIMS Math.*, **9** (2024), 9107–9127. https://doi.org/10.3934/math.2024443

21. I. Lamrani, H. Zitane, D. F. M. Torres, Controllability and observability of tempered fractional differential systems, *Commun. Nonlinear Sci. Numer. Simul.*, **142** (2025), 108501. https://doi.org/0.1016/j.cnsns.2024.108501

22. M. S. Heris, M. Javidi, A predictor-corrector scheme for the tempered fractional diferential equations with uniform and non-uniform meshes, *J. Supercomput.*, **75** (2019), 8168–8206. https://doi.org/10.1007/s11227-019-02979-3

23. T. Zhao, Efficient spectral collocation method for tempered fractional differential equations, *Fractal Fract.*, **7** (2023), 277. https://doi.org/10.3390/fractalfract7030277

24. H. K. Dwivedi, Rajeev, A novel fast tempered algorithm with high-accuracy scheme for 2D tempered fractional reaction-advection-subdiffusion equation, *Comput. Math. Appl.*, **176** (2024), 371–397. https://doi.org/10.1016/j.camwa.2024.11.004

25. A. Bibi, M. Rehman, A numerical method for solutions of tempered fractional differential equations, *J. Comput. Appl. Math.*, **443** (2024), 115772. https://doi.org/10.1016/j.cam.2024.115772

26. M. Partohaghighi, E. Asante-Asamani, O. S. Iyiola, A robust numerical scheme for solving Riesz-tempered fractional reaction–diffusion equations, *J. Comput. Appl. Math.*, **450** (2024), 115992. https://doi.org/10.1016/j.cam.2024.115992

27. S. Duo, Y. Zhang, Numerical approximations for the tempered fractional Laplacian: error analysis and applications, *J. Sci. Comput.*, **81** (2019), 569–593. https://doi.org/10.1007/s10915-019-01029-7

28. H. Zhang, J. Yan, X. Qian, X. Gu, S. Song, On the preserving of the maximum principle and energy stability of high-order implicit-explicit Runge-Kutta schemes for the space-fractional Allen-Cahn equation, *Numer. Algor.*, **88** (2021), 1309–1336. https://doi.org/10.1007/s11075-021-01077-x

AIMS Press

© 2025 the Author(s), licensee AIMS Press. This is an open access article distributed under the terms of the Creative Commons Attribution License (https://creativecommons.org/licenses/by/4.0)